The HKU Scholars Hub The University of Hong Kong 香港大學學術庫

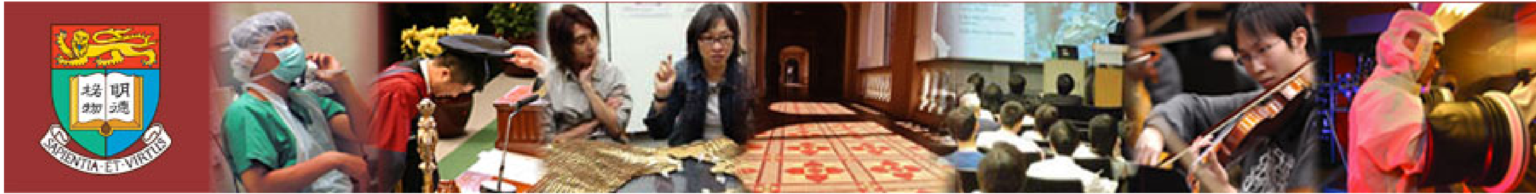

Title	Conduction mechanisms at low- and high-resistance states in aluminum/anodic aluminum oxide/aluminum thin film structure
Author(s)	Zhu, W; Chen, TP; Liu, Y; Fung, SHY
Citation	Journal of Applied Physics, 2012, v. 112 n. 6, article no. 063706
Issued Date	2012
URL	http://hdl.handle.net/10722/169261
Rights	Creative Commons: Attribution 3.0 Hong Kong License

Conduction mechanisms at low- and high-resistance states in aluminum/anodic aluminum oxide/aluminum thin film structure

W. Zhu,[1] T. P. Chen,[1,a)] Y. Liu,[2] and S. Fung[3]
[1]*School of Electrical and Electronic Engineering, Nanyang Technological University, Singapore 639798*
[2]*State Key Laboratory of Electronic Thin Films and Integrated Devices, University of Electronic Science and Technology of China Chengdu, Sichuan 610054, People's Republic of China*
[3]*Department of Physics, The University of Hong Kong, Hong Kong*

(Received 13 March 2012; accepted 15 August 2012; published online 20 September 2012)

In this work, conduction mechanisms of Al/anodic Al oxide/ Al structure, which exhibits resistive switching behavior, have been investigated. The low-resistance state shows ohmic conduction with a metal-like behavior similar to that of pure aluminum. The situation can be explained by the existence of the metallic filament formed by the excess Al in the Al oxide. On the other hand, the high-resistance state (HRS) shows two distinct regimes: ohmic conduction at low fields with a semiconductor-like behavior; and a non-ohmic conduction at high fields. The ohmic conduction of HRS at low fields is attributed to the electron hopping between the states in the oxide with the activation energy of ~0.23 eV. It is suggested that the conduction of HRS at high fields (the maximum voltage is lower than the set voltage) is due to the field-enhanced thermal excitation of the electrons trapped in the states of the metallic Al nano-phase into the conduction band of the Al oxide or the electron emission from the potential well of the metallic Al nano-phase to the conduction band. © *2012 American Institute of Physics*. [http://dx.doi.org/10.1063/1.4754011]

I. INTRODUCTION

Recently, resistive-switching random access memory device (RRAM) has attracted much attention as it opens new possibilities for the next-generation non-volatile random access memory. Various metal oxides such as NiO, TiO_2, Cu_xO, ZnO, and HfO_x have been reported for the RRAM application.[1–11] Up to now, most of the reported works about RRAM have mainly focused on demonstration of memory behaviors and switching mechanisms; few works have investigated the conduction behaviors and conduction mechanisms of the low resistant state (LRS) and high resistant state (HRS).[12–16] A good understanding of the current conduction in different resistance states would help to understand the physics behind the resistive switching phenomena, and it is also necessary to the RRAM applications. Current conduction and resistive switching in aluminum oxide films have been reported in literature.[17–26] In the present work, we have conducted a study of the conduction behaviors of the LRS and HRS in the aluminum/partially anodized aluminum film structure at elevated temperatures. Various conduction mechanisms have been identified based on the temperature and field dependence of the current conduction.

II. EXPERIMENT

A pure Al film with thickness of 500 nm was deposited on a p-type silicon substrate with radio-frequency (RF) sputtering technique. The silicon substrate was first cleaned by piranha and HF solution, and then a 10 nm SiO_2 thin film was thermally grown on the Si substrate by dry oxidation. The purpose of the SiO_2 film is to protect the Si substrate during the anodization process. It should be mentioned that both the SiO_2 film and Si substrate acted as a support only and were not involved in the operation of the resistive switching devices used in the present study. Subsequently, the Al film was anodized in a 0.15 mol/l oxalic acid at room temperature under the application of DC 40 V for about 2 h. During the anodization process, only the Al film connected to the anode was exposed to the acid, while the silicon substrate was kept isolated. As reported in our previous work,[26] the x-ray photoelectron spectroscopy (XPS) measurement indicated that the anodic oxide film was an Al-rich Al_xO_y layer, and the transmission electron microscope (TEM) measurement showed that the Al-rich Al_xO_y layer had the thickness of 30–50 nm. The unreacted Al layer far away from the anodized surface can be regarded as the bottom electrode. After the anodization process, a 300 nm Al film was deposited and patterned on the surface of the anodized Al film as the top electrodes. Thus, a metal-insulator-metal (MIM) structure consisting of Al/anodic aluminum oxide/Al with the pad size of 200 μm in diameter was fabricated on top of the silicon substrate. The electrical measurements were performed between the top and bottom electrodes with the Keithley 4200 semiconductor characterization system equipped with TRIO-TECH TC1000 temperature controller.

III. RESULTS AND DISCUSSION

Figure 1 shows the typical resistive switching occurring during the voltage sweeping in the current-voltage (I-V) measurement at 25 °C. When the voltage reaches the reset voltage (V_{reset}), the current conduction of the MIM structure is switched from a LRS to a HRS; and when the voltage reaches the set voltage (V_{set}), the conduction is switched from the HRS back to the LRS. Figures 2(a) and 2(b) show

a)Electronic mail: echentp@ntu.edu.sg.

 © 2012 American Institute of Physics

Downloaded 19 Nov 2012 to 147.8.230.79. Redistribution subject to AIP license or copyright; see http://jap.aip.org/about/rights_and_permissions

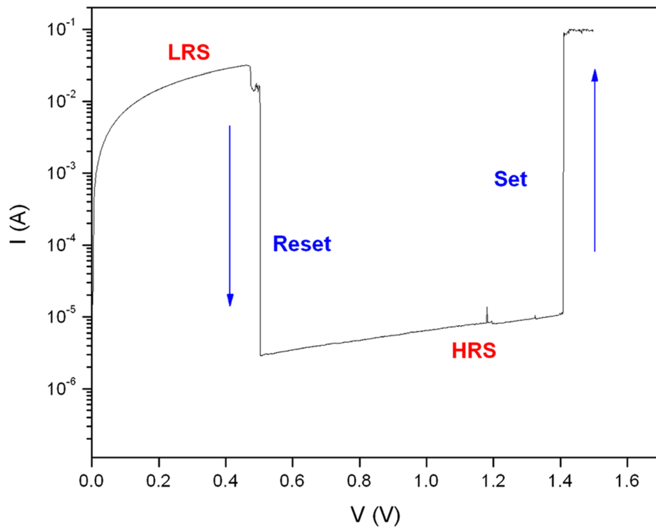

FIG. 1. Reset and set switching occurring during the *I*-*V* measurement at 25 °C.

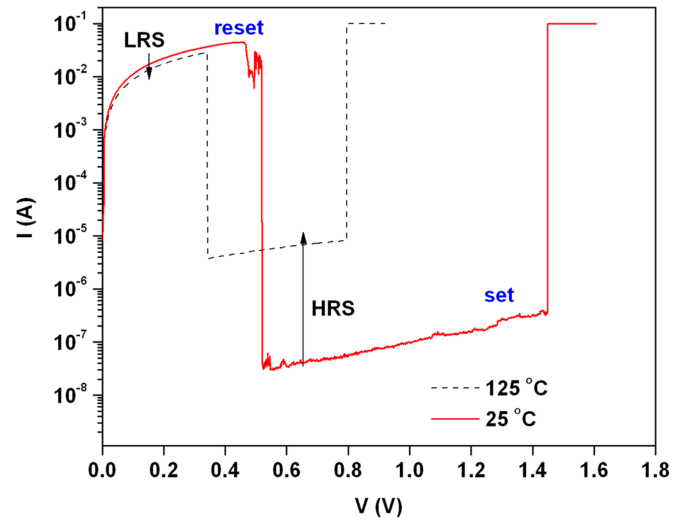

FIG. 3. *I*-*V* measurements with reset and set switching at 25 °C and 125 °C.

the *I*-*V* characteristics measured on the LRS and HRS, respectively, at room temperature (25 °C). Note that the voltages used in the measurements on the LRS and HRS must be lower than the reset voltage and the set voltage, respectively, in order to avoid the occurrence of reset and set switching. As shown in Fig. 2(a), the LRS exhibits perfect ohmic conduction with the resistance of 6 Ω at room temperature. However, as can be observed in Fig. 2(b), the current conduction of the HRS first follows the ohmic law at low fields (the voltage is lower than ~0.4 V) with the resistance of 2.8×10^4 Ω at room temperature and then there is a deviation from the ohmic conduction at high fields (the voltage higher than ~0.4 V). This indicates that there are at least two conduction mechanisms involved in the current conduction of the HRS, depending on the voltage applied.

As can be observed in Figure 3, temperature has a significant effect on the current conduction of both LRS and HRS. As the temperature increases, the current at the LRS decreases while the current at the HRS increases. Figure 4 shows the temperature dependence of the LRS resistance in the temperature range of 25–125 °C. The resistance increases with temperature, showing the behaviour of metal-like conduction. In fact, the resistance is a liner function of temperature with the temperature coefficient of $4.1 \times 10^{-3}\,°C^{-1}$, which is close to the value ($3.9 \times 10^{-3}\,°C^{-1}$) of pure

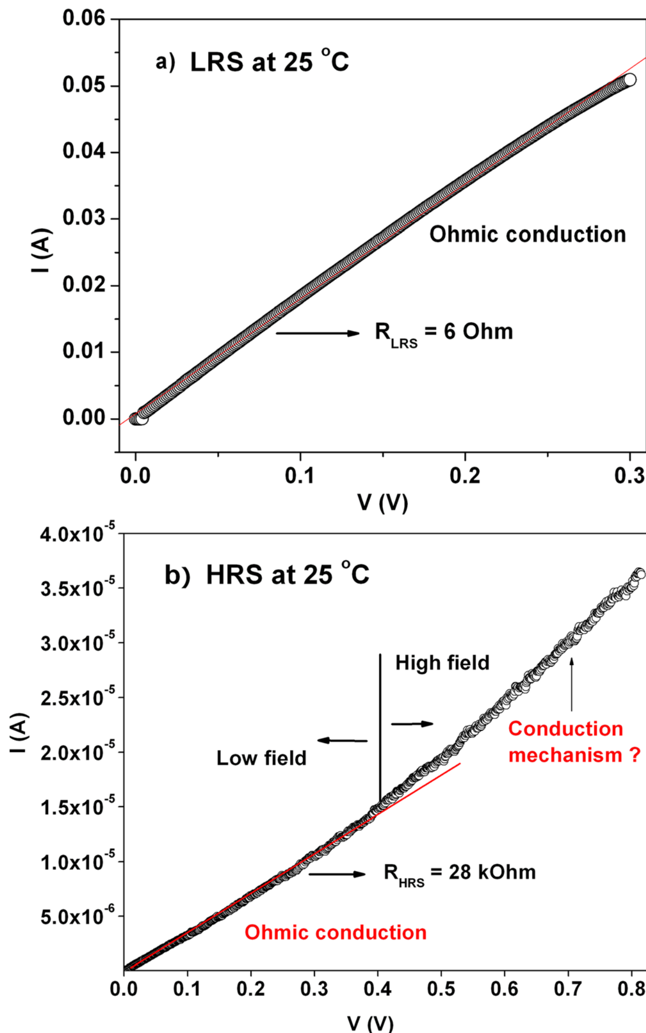

FIG. 2. *I*-*V* characteristics of the two conduction states at 25 °C: (a) LRS and (b) HRS.

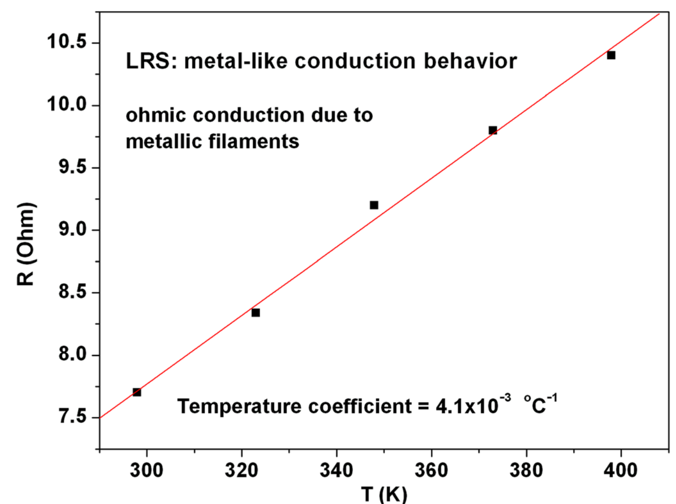

FIG. 4. LRS resistance as a function of temperature.

Downloaded 19 Nov 2012 to 147.8.230.79. Redistribution subject to AIP license or copyright; see http://jap.aip.org/about/rights_and_permissions

aluminum. This suggests that the ohmic conduction of the LRS is due to the existence of the metallic filament formed by the excess Al phase. Note that, as reported in our previous work,[26] there is a high concentration of excess metallic aluminum in the anodized aluminum layer. In this case, as temperature increases, the scattering of the electrons transported in the Al filament by the phonons of the Al phase increases, leading to an increase in the resistance.

In contrast to the metal-like behavior of the ohmic resistance of the LRS, the ohmic resistance of the HRS at low fields exhibits the behaviour of semiconductor-like conduction, i.e., the resistance decreases with temperature, as shown in Fig. 5(a). To understand the semiconductor-like conduction behavior, the Arrhenius plot of the HRS current at the voltage of 0.2 V is shown in Fig. 5(b). The linear plot indicates that the ohmic characteristic is exponentially dependent on temperature, i.e., the resistance $R \sim \exp(\Delta E_a/k_B T)$, where ΔE_a is the activation energy, k_B is the Boltzmann constant, and T is the absolute temperature. The activation energy yielded from the plot is 0.233 eV. Therefore, the current conduction of the HRS at low fields can be explained as follows. In the HRS, although the metallic filament is broken, a small current is carried by thermally excited electrons hopping

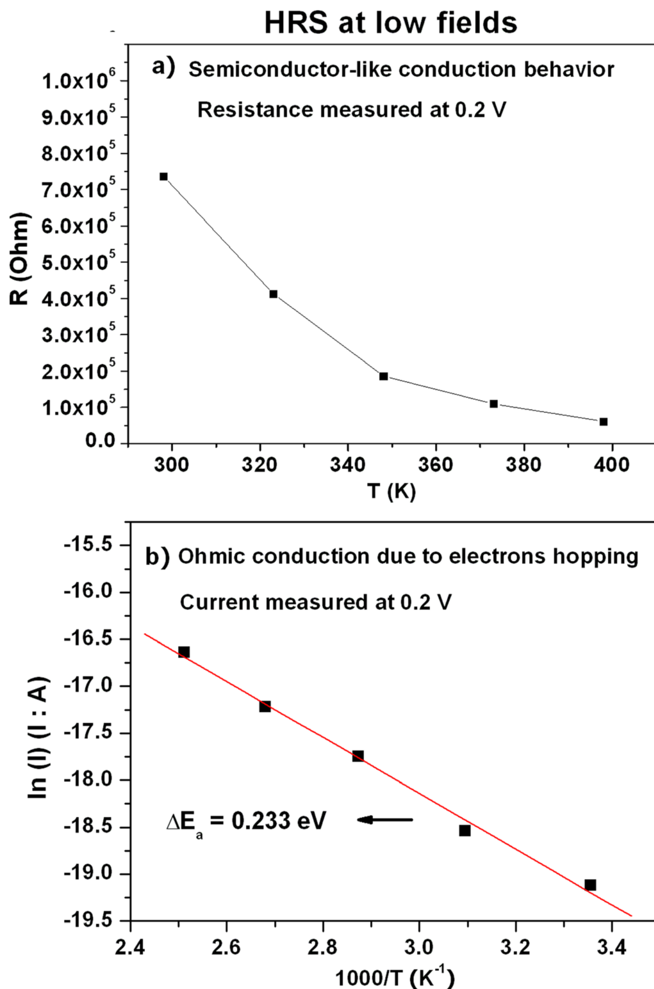

FIG. 5. (a) HRS resistance at a low field as a function of temperature; and (b) Arrhenius plot of the HRS current at a low field. Both the resistance and current measurements were conducted at 0.2 V.

from one state (e.g., the shallow defect states in the Al-rich Al oxide) to the next at low fields at high temperatures, yielding an ohmic conduction. As the thermal excitation process is enhanced at higher temperature, the ohmic resistance decreases with temperature.

As pointed out early, the conduction of the HRS at high fields deviated from the ohmic conduction. The conduction could be limited by a bulk effect or an interface effect.

One of the possible current conduction mechanisms is the Fowler-Nordheim (F-N) tunneling. However, our analysis indicates that F-N tunneling is not the dominant process in the voltage range used in our experiment, as explained in the following. First, the current conduction shows strong temperature dependence. Second, according to the F-N tunneling theory, the F-N plot, $\ln(I/V^2)$ vs. $1/V$ should have a negative slope; however, the F-N plots of our experimental data have positive slopes. Therefore, it can be concluded that F-N tunneling is not the dominant process in the voltage range of the present experiment. Note that the applied voltage must be lower than the set voltage (<1.6 V), otherwise a set switching from the HRS to LRS will occur.

Other possible mechanisms for the conduction of the HRS at high fields could include Poole-Frenkel (PF) emission and Schottky emission (SE). PF emission is a mechanism of bulk effect that is frequently used to describe the leakage conduction in insulators.[27] It is due to field-enhanced thermal excitation of electrons trapped in the insulator (e.g., the Al oxide in the present study) into the conduction band of the insulator. On the other hand, SE is an interface-limited mechanism, which describes the field emission of hot electrons from a metal to the conduction band of an insulator in contact with it.[28] In the Al film/Al-rich Al oxide/Al film structure of the present study, SE can occur at both the oxide/Al film interface and the interfaces between the oxide and the Al nano-phase (e.g., Al nanoparticles) embedded in the oxide. The strong temperature dependence of the conduction of the HRS at high fields observed in the present study suggests that other conduction mechanisms such as the space-charge limited current can be excluded as the main conduction mechanisms. In order to determine whether the PF emission or SE is responsible for the conduction of the HRS at high fields, a detailed data analysis has been carried out, as discussed below.

The current density-voltage (J-V) relationship of the PF emission can be described by[27]

$$J = C\frac{V}{d}\exp\left\{-\frac{q}{\mathrm{k_B T}}\left[\Phi_{\mathrm{PF}} - \sqrt{\frac{\mathrm{qV}}{\mathrm{d}\pi\varepsilon_0\varepsilon_\mathrm{i}}}\right]\right\}, \quad (1)$$

where C is a constant, d is the film thickness, q is electronic charge, $q\Phi_{PF}$ is the depth of the trap's potential well, ε_i is the dynamic dielectric constant, and ε_0 is the vacuum permittivity. According to Eq. (1), $\ln(J/V)$ should be a linear function of $\sqrt{V}$. Indeed, in the small voltage range (the small voltage range is chosen to avoid any switching process), a weak linear dependence of $\ln(J/V)$ on $\sqrt{V}$ is observed, as shown by

Downloaded 19 Nov 2012 to 147.8.230.79. Redistribution subject to AIP license or copyright; see http://jap.aip.org/about/rights_and_permissions

the PF plots in Fig. 6(a). As can be observed in Fig. 6(b), ln(J/V) also shows the Arrhenius behavior for different voltages. The activation energy, $\Delta E_{PF} = q(\Phi_{\rm PF} - \sqrt{\frac{\rm qV}{\rm d\pi\varepsilon_0\varepsilon_i}})$ for the PF emission obtained from the Arrhenius plots is about 0.43 eV for different voltages in the small voltage range. On the other hand, Schottky emission can be expressed as[27]

$$\rm J = A^{*}T^2 \exp\left\{-\frac{q}{k_B T}\left[\Phi_B - \sqrt{\frac{qV}{4\pi d\varepsilon_0\varepsilon_i}}\right]\right\}, \qquad (2)$$

where A^* is a constant and qΦ_B is the barrier height. Obviously, ln(J) should have a linear dependence on $\sqrt{V}$ also. As shown in Fig. 7(a), the SE plots (i.e., ln(J) versus $\sqrt{V}$) indicate that ln(J) indeed increases linearly with $\sqrt{V}$. As shown in Fig. 7(b), ln(J) also exhibits the Arrhenius behavior for different voltages. The activation energies, $\Delta E_{SE} = q\left(\Phi_B - \sqrt{\frac{\rm qV}{4\rm d\pi\varepsilon_0\varepsilon_i}}\right)$ for Schottky emission obtained from the Arrhenius plots at various voltages are about 0.40 eV. Obviously, the field dependence of the activation energies for both PF emission and Schottky emission cannot be clearly observed in the measurements due to the narrow voltage range chosen as a result of avoiding any switching process. Nevertheless, it can be concluded that the activation energies for the PF emission and the Schottky emission are almost the same.

The above analysis indicates that both PF emission and Schottky emission can describe the current conduction of the HRS at high fields in the voltage range used in the present study and have almost the same activation energies. The

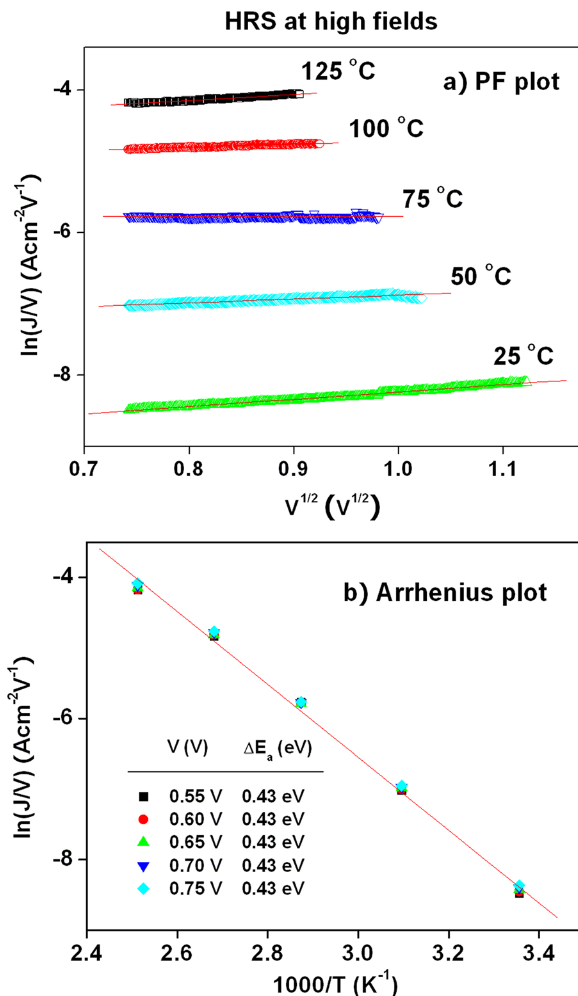

FIG. 6. HRS at high fields: (a) plots of Poole-Frenkel emission at various temperatures; and (b) Arrhenius plots of ln (J/V) at different voltages.

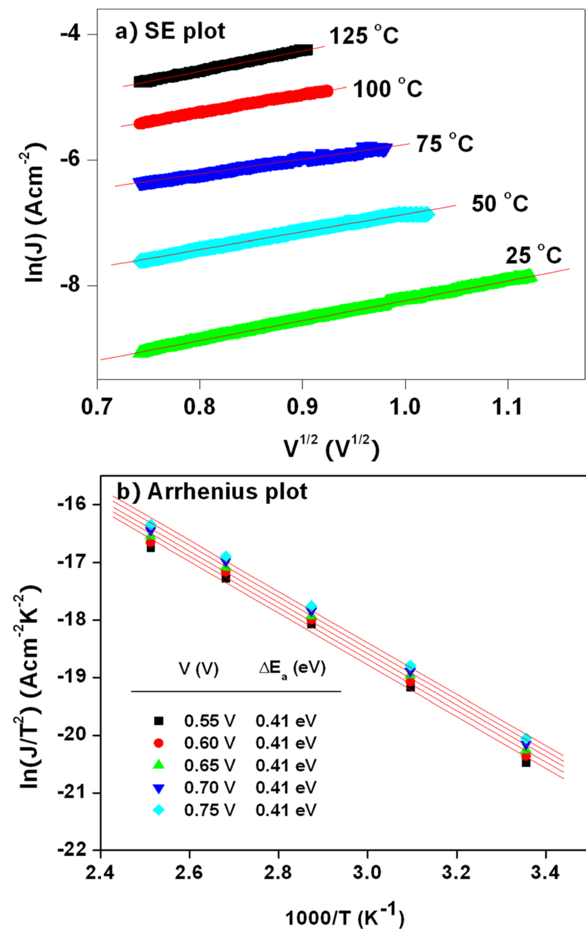

FIG. 7. HRS at high fields: (a) plots of Schottky emission at various temperatures; and (b) Arrhenius plots of ln(J/T^2) at different voltages.

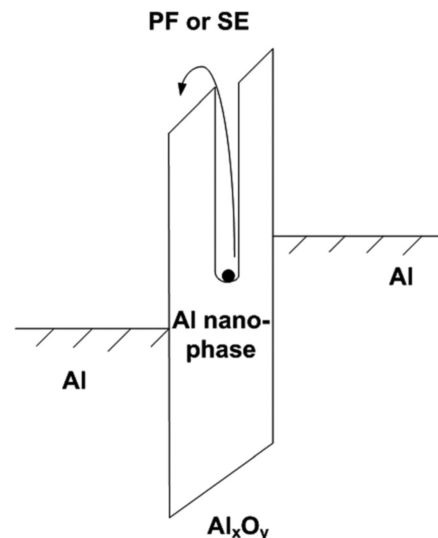

FIG. 8. Schematic diagram for the PF emission or Schottky emission in the system of metallic Al nano-phase embedded in the Al oxide.

Downloaded 19 Nov 2012 to 147.8.230.79. Redistribution subject to AIP license or copyright; see http://jap.aip.org/about/rights_and_permissions

situation can be explained as follows. The metallic Al nano-phase (e.g., Al nanoparticles or nanowires) embedded in the Al-rich Al_xO_y layer plays an important role in the conduction of the HRS at high fields. As shown in Fig. 8, the PF emission can occur due to the field-enhanced thermal excitation of the electrons trapped in the states of the metallic Al nano-phase into the conduction band of the Al oxide. On the other hand, the metallic Al nano-phase forms a potential well, and the electron emission from the potential well to the conduction band of the Al oxide can be described by the Schottky emission.

IV. CONCLUSION

In conclusion, the LRS shows ohmic conduction with a metal-like behavior similar to that of pure aluminum, which can be explained by the existence of the metallic filament formed by the excess Al in the Al oxide. The conduction in the HRS exhibits two distinct regimes: ohmic conduction at low fields with a semiconductor-like behavior; and a non-ohmic conduction at high fields. The ohmic conduction of HRS at low fields is attributed to the electron hopping between the states in the oxide with the activation energy of $\sim$0.23 eV. It is shown that the conduction of HRS at high fields is due to the field-enhanced thermal excitation of the electrons trapped in the states of the metallic Al nano-phase into the conduction band of the Al oxide or the electron emission from the potential well of the metallic Al nano-phase to the conduction band.

ACKNOWLEDGMENTS

This work has been financially supported by National Research Foundation of Singapore (NRF-G-CRP 2007-01). Y. Liu acknowledges the Young Scholar Fund of Sichuan under Project No. 2011JQ0002.

[1]D. Ielmini, F. Nardi, C. Cagli, and A. L. Lacaita, IEEE Int. Reliab. Phys. Symp. Proc. **10**, 620 (2010).
[2]K. M. Kim, M. H. Lee, G. H. Kim, S. J. Song, J. Y. Seok, J. H. Yoon, and C. S. Hwang, Appl. Phys. Lett. **97**, 162912 (2010).
[3]M. Yin, P. Zhou, H. B. Lv, J. Xu, Y. L. Song, X. F. Fu, T. A. Tang, B. A. Chen, and Y. Y. Lin, IEEE Electron Devices Lett. **29**, 681 (2008).
[4]S. Lee, H. Kim, J. Park, and K. Yong, J. Appl. Phys. **108**, 076101 (2010).
[5]U. Russo, D. Ielmini, C. Cagli, and A. L. Lacaita, IEEE Trans. Electron Devices **56**, 186 (2009).
[6]Z. Fang, H. Y. Yu, W. J. Liu, Z. R. Wang, X. A. Tran, B. Gao, and J. F. Kang, IEEE Electron Devices Lett. **31**, 476 (2010).
[7]C. H. Kim, Y. H. Jang, H. J. Hwang, C. H. Song, Y. S. Yang, and J. H. Cho, Appl. Phys. Lett. **97**, 062109 (2010).
[8]H. H. Huang, W. C. Shih, and C. H. Lai, Appl. Phys. Lett. **96**, 193505 (2010).
[9]Y. Sato, K. Kinoshita, M. Aoki, and Y. Sugiyama, Appl. Phys. Lett. **90**, 033503 (2007).
[10]C. Cagli, F. Nardi, and D. Ielmini, IEEE Trans. Electron Devices **56**, 1712 (2009).
[11]A. Chen, S. Haddad, and Y. C. Wu, IEEE Electron Devices Lett. **29**, 38 (2008).
[12]K. Nagashima, T. Yanagida, K. Oka, and T. Kawai, Appl. Phys. Lett. **94**, 242902 (2009).
[13]I. Hwang, M. J. Lee, G. H. Buh, J. Bae, J. Choi, J. S. Kim, S. Hong, Y. S. Kim, I. S. Byun, S. W. Lee, S. E. Ahn, B. S. Kang, S. O. Kang, and B. H. Park, Appl. Phys. Lett. **97**, 052106 (2010).
[14]X. Wu, P. Zhou, J. Li, L. Y. Chen, H. B. Lv, Y. Y. Lin, and T. A. Tang, Appl. Phys. Lett. **90**, 183507 (2007).
[15]M. H. Lin, M. C. Wu, C. H. Lin, and T. Y. Tseng, J. Appl. Phys. **107**, 124117 (2010).
[16]W. Zhu, T. P. Chen, M. Yang, Y. Liu, and S. Fung, Nanosci. Nanotechnol. Lett. **3**, 222 (2011).
[17]T. W. Hickmott, J. Appl. Phys. **33**, 2669 (1962).
[18]T. W. Hickmott, J. Appl. Phys. **88**, 2805 (2000).
[19]T. W. Hickmott, J. Appl. Phys. **104**, 103704 (2008).
[20]J. Song *et al.*, Appl. Phys. Express **3**, 091101 (2010).
[21]Y. Wu, B. Lee, and H.-S. P. Wong, IEEE Electron Devices Lett. **31**, 1449 (2010).
[22]K. M. Kim, B. J. Choi, B. W. Koo, S. Choi, D. S. Jeong, and C. S. Hwang, Electrochem. Solid-State Lett. **9**, G343 (2006).
[23]S. Kim and Y.-K. Choi, Appl. Phys. Lett. **92**, 223508 (2008).
[24]S. Kato, S. Nigo, Y. Uno, T. Onisi, and G. Kido, J. Phys.: Conf. Ser. **38**, 148 (2006).
[25]V. Sh. Yalishev, S. U. Yuldashev, J.-S. Kim, and B. H. Park, Jpn. J. Appl. Phys. Part 1 **48**, 070207 (2009).
[26]W. Zhu, T. P. Chen, Z. Liu, M. Yang, Y. Liu, and S. Fung, J. Appl. Phys. **106**, 093706 (2009).
[27]M. S. Rahman, E. K. Evangelou, I. I. Androulidakis, and A. Dimoulas, Electrochem. Solid-State Lett. **12**, H165 (2009).
[28]P. R. Emtage and W. Tantraporn, Phy. Rev. Lett. **8**, 267 (1962).

Downloaded 19 Nov 2012 to 147.8.230.79. Redistribution subject to AIP license or copyright; see http://jap.aip.org/about/rights_and_permissions